Modular Cloning Tools for Streptomyces spp. and Application to the De Novo Biosynthesis of Flavokermesic Acid

Jean-Malo Massicard, Delphine Noel, Andrea Calderari, André Le Jeune, Cyrille Pauthenier, Kira Weissman

Modular Cloning Tools for *Streptomyces* spp. and Application to the *de novo* Biosynthesis of Flavokermesic Acid

Jean-Malo Massicard[1], Delphine Noel[1], Andréa Calderari[1], André Le Jeune[2], Cyrille Pauthenier[2] and Kira J. Weissman[1]

[1]Université de Lorraine, CNRS, IMoPA, F-54000 Nancy, France

[2]Abolis Biotechnologies, 5 Rue Henri Auguste Desbruères Bâtiment 6, 91000, Évry

E-mail: kira.weissman@univ-lorraine.fr

ABSTRACT: The filamentous *Streptomyces* are among the most prolific producers of bioactive natural products, and are thus attractive chassis for the heterologous expression of native and designed biosynthetic pathways. Although suitable *Streptomyces* hosts exist, including genetically-engineered cluster-free mutants, the approach is currently limited by the relative paucity of synthetic biology tools facilitating *de novo* assembly of multi-component gene clusters. Here, we report a modular system (MoClo) for *Streptomyces* including a set of adapted vectors and genetic elements which allow for construction of complete genetic circuits. Critical functional validation of the each of the elements was obtained using the previously-reported β-glucuronidase (GusA) reporter system. Furthermore, we provide proof-of-principle for the toolbox in *S. albus*, demonstrating efficient assembly of a biosynthetic pathway to flavokermesic acid (FK), an advanced precursor of the commercially valuable carminic acid.

KEYWORDS: *Streptomyces*, natural product, anthraquinone, modular cloning, synthetic biology.

■ INTRODUCTION

Although *Escherichia coli* and *Saccharomyces cerevisiae* (baker's yeast) remain the work-horse organisms for routine synthetic biology, multiple species of *Streptomyces* have also attracted interest as chassis.[1,2] Indeed, the *Streptomyces* exhibit multiple favorable traits, including their rich and varied specialized metabolism, as well as their amenability to metabolic engineering strategies geared towards yield improvement.[3] Nonetheless, such efforts are currently hampered by the relative lack of genetic tools required to assemble in combinatorial fashion and functionally validate extended sets of biosynthetic genes.

Work in this direction has recently focused on engineering platforms for the biosynthesis of a variety of aromatic polyketides of both therapeutic and industrial interest.[4,5] These pathways include a minimal set of polyketide synthase (PKS) enzymes required to construct a linear, poly-β-ketone chain of variable length (**Figure 1**): a ketosynthase α (KS_α)/KS_β heterodimer responsible for initiation of the assembly process and repeated rounds of Claisen-like chain extension, and an acyl carrier protein (ACP) to which the growing chains are tethered. The required building blocks are furnished by an enzyme borrowed from fatty acid biosynthesis, the malonyl CoA:ACP transacylase (MCAT).[6] The minimal PKS collaborates with additional enzymes to optionally reduce (ketoreductase (KR)) and regiospecifically cyclize/aromatize (CYC/ARO) the intermediates to form the characteristic aromatic core structures.[7]

To date, the most successful efforts at pathway reconstruction have focused on intact operons derived from native biosynthetic gene clusters (BGCs), coupled with promoter engineering and the use of expression vectors optimized for various *Streptomyces* strains.[4,5] However, alternative approaches (e.g. Golden Gate,[8] and modular cloning methods such as MoClo[9] and/or GoldenBraid[10]) must be employed when the aim is to assemble several transcription units (TUs) from diverse sources, including non-actinomycete genomes and/or synthetic genes. The use of synthetic genes, in particular, allows for codon optimization[11] which may be necessary for efficient expression of heterologous genes in *Streptomyces*.[4,12] In this vein, an assembly method derived from the Golden Standard toolkit (a Type IIS assembly method based on the Standard European

Vector Architecture (SEVA)[13]) was recently employed to produce the hydroxylated flavonoid eriodyctiol in *S. albidoflavus*,[14] using a type III PKS and associated decorating enzymes. However, expanding the potential of this strategy depends on identifying additional genetic elements (promoters-ribosome binding sites (RBSs), CDSs and terminators), which can be easily deployed in a 'plug-and-play' manner in diverse *Streptomyces* strains.

Towards this end, we report here an expanded synthetic biology toolkit for *Streptomyces* and other actinomycetes based on the previously-reported pOSV series of integrative plasmids,[15] which allows both for rapid functional validation of genetic elements, and their integration into streamlined genetic circuits. As proof-of-concept, the system was leveraged to synthesize the anthraquinone flavokermesic acid (FK) **1** (**Figure 1**) (also named TMAC[16]), a precursor to the industrially relevant carminic acid, in both *S. albus* J1074 and *S. lividans* TK24.[1] For this, we used two distinct combinations of native type II PKS components (AntDEFBG (AQ256)[17–19] and NcnABC (napthocyclinone)[20,21]), coupled with suitable sets of tailoring enzymes. In total, the genetic circuits comprise 7 heterologous TUs, demonstrating the utility of our approach for generating operational multi-gene assemblies.

■ RESULTS AND DISCUSSION

Choice of the Test Biosynthetic System and *Streptomyces* Strains. Carminic acid (CA) **2** is a *C*-glycosylated anthraquinone which is widely used in the pharmaceutical, food and cosmetics industries as a bright red colorant.[22,23] While the natural origin of CA in scale insects[23] remains a mystery apart from the terminal insect-derived *C*-glycosyl transferase,[24] the pathway incorporates an FK intermediate **1** (**Figure 1**) which can be accessed via classical polyketide biochemistry in combination with two cyclase/aromatase (CYC/ARO) enzymes which afford the flavokermesic acid anthrone (FKA) **3** core, followed by C-6 oxidation.[23] FK is then transformed to carminic acid **2** via the action of a C-8 hydroxylase which yields kermesic acid (KA) **4**, followed by the *C*-glucosyltransferase (*C*-GT) (**Figure 1**). To date, CA has been obtained heterologously from *E. coli*[19] and two fungal species, *Aspergillus nidulans*[25] and *Saccharomyces cerevisiae*[12], using alternatively a type II PKS (AntDEFBG from the bacterium *Photorhabdus luminescens*) or type III PKS (OKS from the plant *Aloe arborescens*) to synthesize the required octaketide poly-β-ketone chain **5**. In all cases, cyclization and aromatization to afford the FKA **3** core were achieved using the enzyme pair ZhuI/ZhuJ from the R1128 polyketide pathway of *Streptomyces* sp. R1128.[16,26] It has previously been demonstrated, however, that *S. coelicolor* CH999, a strain engineered to lack the actinorhodin (*act*) cluster,[27] expressing both the *act* minimal PKS and ZhuI/ZhuJ, gives rise to FK **1**. However, the yields of **1** were 2-fold reduced relative to the shunt products Sek4 **6a** and Sek4b **7a** (**Figure 1**).[16] The incomplete flux towards FK may have been due to sub-optimal interactions between the Act minimal PKS and the R1128-derived ARO/CYC enzymes, or the fact that the octaketide **5** bearing an acetate starter unit is not the natural substrate of the two cyclases. In any case, these data argued for the utility of FK biosynthesis as a test bed for our synthetic biology platform.

In terms of hosts, we selected *S. albus* J1074 and *S. lividans* TK24. *S. albus* J1074 is a mutant of the *S. albus* G strain lacking the *Sal*I restriction/modification system, and which grows rapidly relative to other *Streptomyces* species.[1] In addition, genetic tools (e.g. replicative/stably integrative vectors, promoters/terminators/reporter genes, conjugation protocols, etc.) for manipulating the strain are well developed, and indeed, it has been used successfully to express a large number of heterologous pathways.[1] Production titers are also often higher from *S. albus* than *S. coelicolor* and *S. lividans*, potentially due to the presence of two highly active *attB* phage integrase sites in the *S. albus* genome.[1] *S. lividans* TK24 is also one of the most genetically tractable actinobacteria.[28] Notably, it accepts methylated DNA, has low endogenous protease activity, and contains a mutation conferring streptomycin resistance which improves production of specialized metabolites. The *act*

pathway is encoded in its genome, and an *actVI-orf1* (Act KR) mutant of *S. coelicolor* has been shown to produce DMAC (3,8-hydroxy-1-methyl-anthraquinone-2-carboxylic acid),[27,29] a close relative of FK **1** (Note: DMAC differs from TMAC via C-9 ketoreduction prior to cyclization/aromatization). *S. lividans* was therefore a potential source of the shunt metabolites Sek4 **6**, Sek4b **7** and mutactin **8** (**Figure 1**), and thus a useful control strain for the engineered *S. albus*.

Development of the Modular Expression System. With the target biosynthetic pathway identified, the first goal was to develop a flexible system for modular cloning in *Streptomyces* based on a hierarchical assembly of functional DNA parts into genetic circuits using receptor vectors from levels 0–2 (**Table S1**).[8,9] To build the level 0 promoter-RBS, CDS and terminator parts, DNA fragments were obtained by PCR amplification, oligonucleotide annealing and chemical synthesis (**Tables S2–S6**). As necessary, we domesticated the DNA fragments by removing native *Bbs*I and *Bsa*I recognition sites,[11] and all fragments were cloned with high efficiency into an acceptor vector (Zero Blunt™ from Invitrogen™). The overall result was to obtain level 0 parts flanked by *Bbs*I restriction sites and incorporating five unique four-nucleotide fusion sites (labeled A–E in **Figure 2**). By respecting the fusion site syntaxes, promoter-RBS A(*CGAT*)B(*AATG*), CDS B(*AATG*)D(*AGTG*) and terminator D(*AGTG*)E(*GACA*) parts were successfully assembled using one-pot restriction and ligation reactions into transcription units (TUs), such that no *Bbs*I recognition sites remained in the final level 1 constructs. The intrinsic flexibility of this strategy means that additional genetic elements (e.g. signal peptides, N-terminal or C-terminal solubility/purification tags, etc.) could be added, as desired.

To facilitate the variable positioning of the engineered TUs in more complex genetic circuits, we developed seven level 1 receptor vectors containing a chloramphenicol resistance cassette, and flanked with the *Bbs*I sites and additional *Bsa*I sites to allow assembly of up to 4 TUs in a final level 2 host vector (**Figure 2** and **S1**). The employed level 2 vectors are derived from the previously-described plasmids pOSV802 and pOSV811 developed by Aubry *et al.*, which have already been used in several *Streptomyces* hosts including *S. lividans* TK23 and *S. albus* J1074.[15] These vectors differ from each other in terms of the selection markers and sites of integration into *Streptomyces* genomes (pOSV802 = Apr^R + ΦC31; pOSV808 = Hyg^R + VWB; pOSV811 = Kan^R + pSAM2). For application here, we domesticated the plasmids in order that only two *BsaI* sites were present flanking the selection cassette (**Table S1**), and in addition replaced the blue chromoprotein-based selection cassette with that encoding the yellow fluorescent protein (YFP)[30] under the control of *lacP*, allowing for more rapid visualization of negative clones (**Figure 2**). Ultimately, only the vector derived from pOSV802 was used in this study.

The assembly of level 2 constructs occurs in a fixed and directional order through the fusion sites 1–4 generated by *Bsa*I digestion (**Figure 2**). In contrast to other MoClo systems with a single level 2 receptor vector that require linker parts to fill empty positions, the library of level 2 vectors arising from modular cloning significantly increases assembly simplicity by avoiding the use of extra adapters. To accommodate cases where it is desirable to assemble only a single transcription unit (promoter-RBS, CDS and terminator), we engineered a third level 2 acceptor vector based on pOSV808[15] which was domesticated to allow for direct introduction of level 0 parts via two remaining *Bbs*I restriction sites, again flanking the YFP selection cassette. This vector can also accommodate TUs pre-assembled into pOSV802 and pOSV811, and obtained by PCR amplification of the TU-encoding region using primers containing *Bbs*I sites. All level 2 acceptor vectors contain a prefix (*Avr*II and *Nhe*I sites) and a suffix (*Avr*II and *Spe*I sites) flanking the modular cloning cassette, allowing for the introduction of further modifications by traditional restriction enzyme-based cloning.[15]

Concerning the choice of promoters, it has been argued that they should fit within a single primer to simplify engineering, should have an identified transcriptional start site, and function constitutively to ensure relatively equal expression levels of all genes.[1] The promoters used in multi-gene constructs should also be sufficiently divergent in terms of

sequence composition to avoid unwanted recombination. For this work, we chose to assemble and test a 21-membered promoter collection (**Table S3**), based on a number of sequences recently described to work in *Streptomyces* spp.[31–35] One set included 5 promoters associated with expression of the glycolytic enzymes GAPDH (*gapdhp* from *S. lividans* (SL), *S. griseus* (SG) and *Eggerthella lenta* (EL)), enolase (*enop* from *S. lividans*) and fructose biphosphate aldolase (*fbap* from *S. lividans*), as well as *rpsLp* of *Xylanimonas cellulosilytica* (XC), the promoter of the 30S ribosomal protein S12. We notably selected the *gapdhp* of *E. lenta* and *rpsLp* of *X. cellulosilytica* because these promoters were used in vector pCRISPomyces-2 which permits efficient CRISPR-based engineering of various *Streptomyces* strains.[36] We also tested five of 10 constitutive promoters identified from *S. albus* J1074 (i.e. *pXNR_3799*, *pXNR_1700*, *pXNR_4375*, *pXNR_3720* and *pXNR_3170*), which are stronger than the widely used constitutive promoter *ermE*p* from *Saccharopolyspora erythraea*, as measured by both enzymatic assay and transcriptional analysis.[33]

We also chose to evaluate the *kasOp** promoter, a simplified version of the parental *kasOp* engineered by removing multiple binding sites for the activator ScbR and the repressor ScbR2.[37–39] *kasOp** was also shown to exhibit stronger activity than *ermE*p* in three species of *Streptomyces* at both the transcriptional and protein levels, and used to drive the expression of *actII-ORF4* in *S. coelicolor*, resulting in increased actinorhodin production.[39] To address the issue of balanced transcription, we also utilized three members (i.e. *A09p*, *A15p* and *A26p*) of a promoter library derived from *kasOp** developed by Ji *et al.*,[32] which all permitted a comparable level of expression as the parental *kasOp** but via non-redundant sequences. The function of these promoters was notably validated by refactoring of the actinorhodin biosynthetic gene cluster expressed heterologously in *S. albus* J1074.[32] Similarly, we chose P*tac*RBS3*, P*lac*RBS3*, P*tet*RBS3*, which were engineered to achieve at once both high transcription and high translation in *S. lividans* TK24.[35] Finally, we tested *tipAp* as an example of an inducible promoter which is widely used in *Streptomyces* engineering,[40] and the synthetic promoter *SP44p* which was previously employed to activate production of the cryptic metabolite lycopene in *S. avermitilis*.[31]

We next turned our attention to gene terminators, only a few of which are routinely used by the community for plasmid engineering in *Streptomyces*.[41,42] Although the impact of terminators is relatively minor compared to promoters and the regions surrounding the RBS, they nonetheless constitute an important component of genetic circuits. Two types of terminators have been identified to function in prokaryotes: factor-dependent terminators, which rely on the special regulatory protein Rho, and factor-independent terminators, which do not require any additional protein cofactors to terminate transcription. The latter type is evidently better adapted to synthetic biology applications.[43,44] For simplicity and to avoid the repeated use of single terminators in our genetic circuits, we opted to use 10 terminators published previously.[4,15,36,45]

In order to assess our choice of genetic elements, we constructed three level 2 vectors permitting screening of gene expression based on glucuronidase (GusA) activity (**Figure 3A**). Quantification of the promoter-RBS parts (**Figure 3B**) using pOSV808m-P (**Figure S2**) showed that *gapdhp(EL)* and *rpsLp(XC)* have similar activities. Likewise, *kasOp**, *A09p*, *A15p* and *A26p* which were shown previously to exhibit higher activity than *ermE*p* via quantification of indigoidine,[32] were active at similar levels as *gapdhp(EL)* and *rpsLp(XC)* in our study. Surprisingly, *Ptet*RBS3* that has been described to have approximately 7-fold normalized strength relative to *kasOp** using the *gusA* reporter gene,[35] did not lead to substantially higher relative expression under our conditions. Evidently, stronger promoter activity does not always maximize gene expression, as other factors can come into play (e.g. a non-optimal combination of promoter-RBS and CDS and/or the metabolic burden imposed on the heterologous host). *ptipA* (induced with 1 µM of thiostrepton) and *SP44p* showed similar activity in both *S. lividans* and *S. albus*, and of the same magnitude as the other promoters tested. Overall, these results demonstrated that the assembled promoter collection gave similar levels of expression as judged by the GusA reporter

system (**Figure 3B**). Concerning the tested terminator parts, all were shown to be functional with no substantial variation of glucuronidase activity, and thus they are also interoperable (**Figures 3C** and **S2**).

Engineering a Genetic Circuit for *de novo* Flavokermesic Acid Biosynthesis. We initially deployed our modular cloning system with several transcription units for FKA (**3**) biosynthesis. The first of these was based on the recent successful reconstitution of carminic acid biosynthesis in *E. coli*.[19] In this case, the core anthraquinone was assembled by a set of proteins from the AQ-256 pathway of *Photorhabdus luminescens* TT01.[18] These include AntBDEFG (AntD–F = minimal PKS; AntD = KS_α; AntE = KS_β; AntF = ACP), *antB* (AntB = phosphopantetheinyl transferase necessary for post-translational activation of AntF), and *antG* (AntG = CoA ligase)), which were used in combination with the ARO/CYC pair ZhuI and ZhuJ from *Streptomyces* R1128. To reconstitute an equivalent system, we obtained all of the necessary genes by gene synthesis in codon optimized version (Integrated DNA Technologies, USA), based on the native codon preference of *S. coelicolor*. We also domesticated the DNA sequences of genes *zhuI* and *zhuJ*[46] by overlap PCR to remove *Bbs*I/*Bsa*I recognition sites, while maintaining the natural *Streptomyces* operon structure in order not to alter translation initiation. The second system tested was the minimal PKS NcnA–C and the CYC/ARO pair NcnD/NcnE from the napthocyclinone type II PKS of *S. arenae* DSM 40737,[21] as the equivalent genes from *S. eurocidicus* CGMCC 4.1086 were shown previously to function in *S. albus* J1074.[20] No codon optimization was necessary in this case given the *Streptomyces* origin of the genes, but *ncnD* and *ncnE* were domesticated to remove *Bbs*I/*Bsa*I recognition sites. The native operon sequence of *ncnABC* was amplified from the gDNA as two regions of 833 bp and 2023 bp, which were then assembled by overlap PCR while simultaneously introducing a G834C mutation into *ncnA* to remove a *BbsI* recognition site (**Table S2**).

Prior to assembly of the genetic circuits (**Figure 4A**), we employed the pOSV808m-CDS (**Figure S2**) to control the expression of each individual CDS as well as the *zhuI*/*zhuJ* and *ncnA–C* operons in both *S. lividans* and *S. albus*, under control of their associated promoters (**Figure 3D**), using CDS B(*AATG*)C(*GAAG*) syntax. It must be noted that we do not claim to have identified the 'optimal' promoter/CDS combinations, but only those which were broadly functional. In any case, only the ZhuJ expression system resulted in relatively lower GusA activity, which we presume reflects the fact that *zhuJ* has been translationally decoupled from *zhuI*. It may thus in certain cases be desirable to maintain native transcription units, even if this architecture reduces the ability to control the expression of the individual genes. Evidently, the relative merits of the two approaches can be assessed directly using proteomics to measure levels of the expressed proteins.

Having validated the expression of all of the target proteins (**Figure 3D**), we next evaluated the functionality of the Ant and Ncn minimal PKSs. In the absence of CYC/ARO enzymes, we anticipated that minPKS expression would lead to the formation of Sek4 **6a**, Sek4b **7a**, and their respective dehydrated forms (**6b** and **7b**), and potentially to mutactin **8a**/dehydro-mutactin **8b** if the strains harbored a promiscuous KR activity (**Figure 1**).[25,47] In the case of the Ant system, plasmids pOSV802m-*antBDEF* and pOSV808m-*antG* (**Figures 4A** and **S3**) were constructed to include promoters that gave comparable GusA levels, as a proxy for protein expression, in order to balance the levels of the encoded proteins. The plasmids were then introduced into *S. albus* J1074 and *S. lividans* TK24 by conjugative transfer (for all strains generated in this study see **Table S7**). Integration of the vectors into the genomes via ΦC31 and VWB-sites[15] was verified by colony PCR, and then each strain was cultivated in MYG media for 5 days. Analysis of culture extracts was then carried out by LC-HRMS/MS, using untransformed wild type strains and wild type transformed with empty vector as controls. The obtained data were compared to previously published data for FK **1**, and **6**–**8**.[19,21,25,27,47–49]

In the case of wild-type *S. albus* J1074, no *m/z* $[M+H]^+$ corresponding to the compounds of interest **1**–**8** were detected (**Figure 4B**), and thus this strain was ideal for evaluating the functionality of the type II PKS genetic circuits. Introduction of

the AntBDEFG TUs in *S. albus* incorporating the pre-validated promoter-RBS/CDS combinations, resulted in detectable formation of Sek4 **6a** and/or Sek4b **7a** ($C_{16}H_{14}O_7$, retention time (r.t.) 10.07 min; *m/z* = 319.0812 $[M+H]^+$; Δ ppm = −1.5) (**Figures 4B,C** and **S7, Table S8**) and their corresponding dehydrated forms **6b** and/or **7b** ($C_{16}H_{12}O_6$, r.t. 10.51 min; *m/z* = 301.0707 $[M+H]^+$; Δ ppm = −2.7) (**Figures S8** and **S9**) as expected, validating the engineered system. (Note: under our conditions a single peak was observed at 10.07 min, which on the basis that dehydrated forms of **6a** and **7a** were both observed (**Figures S8** and **S9**), likely corresponds to a mixture of Sek4 and Sek4b).

Analysis of WT *S. lividans* TK24 revealed peaks consistent with all three shunt metabolites **6**–**8** in both non- and dehydrated forms (mutactin **8a** ($C_{16}H_{14}O_6$; r.t. 10.43 min; *m/z* = 303.0863 $[M+H]^+$; Δ ppm = −3.2); dehydro-mutactin **8b** ($C_{16}H_{12}O_5$; r.t. 10.40 and 11.14 min (keto-enol tautomers); *m/z* = 285.0757 $[M+H]^+$; Δ ppm = +0.7)) (**Figures S5** and **S6, Table S9**), confirming its utility as a control. We attribute this finding to the presence in the strain of a complete Act pathway, for which evidently flux to actinorhodin is incomplete. Although the metabolic background of *S. lividans* TK24 was complex, we could nonetheless identify production of FK **1** upon introduction of AntBDEFG (**Figures 4B,C**, and **S11, Table S9**). Reasoning that endogenous hydroxylase present in the strain[50] might act on FK **1** to yield kermesic acid **4**, we also searched for peaks corresponding to **4** ($C_{16}H_{10}O_8$; *m/z* = 331.0448 $[M+H]^+$; Δ ppm = +0.9). For this, we used as a **4** standard a commercial extract of carminic acid, within which a minor amount of **4** was present (r.t. 11.76 min) (**Figure S12**). While we did not detect a peak at the corresponding retention time, we did identify a peak at r.t. 10.81 min with the same exact mass, which could thus represent a kermesic acid isomer. However, additional data will be required to verify this hypothesis. It is also curious that **1** and the **4** isomers were not observed in the wild type extracts, but it is likely that their yields were below the limits of detection under our conditions.

We next inserted *ncnA*–*E* into the Level 2 vector pOSV808m under alternative control by *gapdhp(EL)* or *pkasOR15* promoter-RBS sequences, and with a Fd terminator, resulting in vectors pOSV808m-*gapdhp*(EL)-*ncnABC-Fd* and pOSV808m-*pkasOR15-ncnABC-Fd*, respectively (**Figure S4**). These vectors were then introduced into *S. lividans* TK24 and *S. albus* J1074, and growth extracts analyzed by LC-HRMS/MS as described above. This analysis revealed an increase in the production of FKA **1** in *S. lividans* as judged by the relative peak areas, but none of **1**–**8** in *S. albus*. This result was surprising, given that expression of *ncnABC* in *S. coelicolor* CH999 resulted in the production of Sek4 **6a** and mutactin **8a**.[21] A potential explanation was provided by the recent discovery of a second napthocyclinone cluster in *S. eurocidicus* CGMCC 4.1086, which prompted the authors to assign the full gene set present in *S. arenae* DSM 40737.[20,21,51] This analysis identified in addition to the minimal PKS genes *ncnA*–*C*, and the ARO/CYC-encoding genes *ncnD* and *ncnE*, a gene *ncnL*. *ncnL* encodes an acetyl-CoA ligase, an activity reminiscent of AntG from the AQ256 pathway. This observation suggests that the biosynthesis is initiated directly from acetate[17] as opposed to via decarboxylation of ACP-tethered malonate. In any case, the absence of *ncnL* from the expression construct and that of a pathway-specific PPTase, as well as the potential inability of the *S. albus* MCAT to interact with the Ncn ACP to furnish extender units, could explain the failure of the minimal PKS to function in *S. albus*.

We next evaluated whether we could functionally extend the pathway to incorporate the cyclization/aromatization steps. For this, we constructed vectors pOSV808m-*antG-zhuI-zhuJ*, pOSV808m-*antG-zhuIJ* and pOSV808m-*antG-ncnD-ncnE* (**Figure 5A**), and introduced them into *S. albus* and *S. lividans* containing the AntBDEF system. The difference between the first two vectors is that in the second, *zhuI* and *zhuJ* are translationally coupled, which allowed assessment of whether the natural operon structure is important. The genetic character of the strains was verified by colony PCR against the full set of genes present in each plasmid, and cultivated in MYG media for 5 days, followed by analysis by LC-HRMS/MS. LC-HRMS/MS analysis of *S. albus* extracts revealed that the presence of ZhuI and ZhuJ resulted in addition to Sek4 **6** and Sek4b **7**, biosynthesis of FK

1 (**Figure 5B,C**), consistent with results obtained upon expression of the same gene set in *E. coli*.[19] Concerning NcnD and NcnE, this ARO/CYC couple was shown previously to produce DMAC when co-expressed with the actinorhodin minimal PKS and Act KR.[21] Our successful detection of **1** (**Figure 5B,C**) in *S. albus* demonstrates that the enzymes can also act on C-9 unreduced octaketide chain. Introduction of the two enzymes did not substantially alter the metabolic profile in *S. lividans*, for which we observed FK **1** even in the absence of added cyclases (**Table S9**).

■ CONCLUSIONS

In this work, we aimed to address the lack of a modular cloning toolbox for *Streptomyces*, to underpin the increased exploitation of these species as heterologous hosts for specialized metabolite biosynthesis. To this end we developed a three-level MoClo system, and demonstrated its utility in two different *Streptomyces* strains (*S. lividans* TK24 and *S. albus* J1074). The engineered constructs include L0 vectors harboring 10 promoters and 10 factor-independent terminators, L1 vectors hosting complete transcription units (promoter-RBS-CDS-terminator), and three L2 vectors based on the pOSV series[15] capable of housing up to four previously assembled TUs in a defined order. We further improved the L2 backbone by swapping the blue-chromoprotein-based selection for a yellow fluorescent protein, and the vectors incorporate prefixes/suffixes permitting further facile gene additions.

The promoters and terminators were functionally validated using the GusA (glucuronidase) reporter assay, and shown to give comparable expression levels. Therefore, members of this toolbox can be employed interchangeably for achieving balanced protein expression in *Streptomyces*. We then utilized our system to progressively construct a multi-component pathway to the anthraquinone flavokermesic acid **1**, by initial expression of two heterologous minimal type II PKSs Ant and Ncn, followed by addition of an aromatase/cyclase pair, ZhuI/ZhuJ, from a third type II PKS pathway. In the case of the *Streptomyces arenea*-derived Ncn system, the native operon structure of the minimal PKSs genes was maintained, while in the case of the Ant PKS of *Photorhabdus*, each of the minimal PKS genes was under the control of a separate promoter. Expression of the target proteins was confirmed in all cases, and both reconstituted systems resulted in the expected range of products as judged by LC-HRMS/MS and comparison to published data. This result confirmed that it is not always necessary to maintain the native operon structure of type II PKS systems to achieve metabolite production.

Overall, our experiments also bolster the idea that certain type II PKS pathway enzymes exhibit substrate promiscuity.[19,25,29] Notably, the homologous NcnD and NcnE were capable of recognizing C_{16} substrates lacking the native C-9 hydroxyl groups, a result which echoes the ability of Act ARO/CYC ActVII (SCO5090) and ActIV (SCO50911) to similarly act on non-reduced substrates in engineered strains.[16,27,52] Interestingly, these results do not accord with a previous suggestion that ARO/CYC enzymes segregate strictly into two subclasses: those acting on nonreduced poly-β-ketone substrates, and those which recognize C–9 reduced poly-β-ketone intermediates.[53] Similarly, an endogenous hydroxylase apparently recognized FK **1** as a substrate, giving rise to an isomer of kermesic acid **4**. Taken together, these results argue for the utility of these particular enzymes for the engineered biosynthesis of polycyclic aromatic polyketides and their derivatives.

In conclusion, the extensive modular genetic toolbox developed here should substantially advance *Streptomyces* synthetic biology, furthering efforts both in genome mining[54,55] and advanced *de novo* pathway construction.[1,3]

■ Methods

Strains, Plasmids, DNA Sequences and Chemicals. *Streptomyces albus* J1074 and *Streptomyces lividans* TK24 were used as the hosts for engineering. *E. coli* DH5α was used for plasmid construction, propagation and gene maintenance. *Streptomyces arenae* DSM 40737 was employed for isolation of gDNA and amplification of the *ncn* genes. Synthetic, codon-

optimized genes encoding AntBDEFG, ZhuIJ and NpgA were obtained by IDT™. Codon optimization was performed *via* the codon utilization tool from IDT™ using *Streptomyces coelicolor* as a reference. The list of optimized and synthetic genes is provided as **Table S2**. Plasmid PCR™-Blunt (Invitrogen™), P12/P15/P23/P25/P34/P35/P45 (our unpublished results), and pOSV802m/pOSV808m[15] were employed for plasmid construction and gene expression in *Streptomyces*. All other chemicals were purchased from Sigma-Aldrich™ and Thermo Scientific™.

Construction of Plasmids and Strains. All genes used in this study were amplified by PCR using Phusion™ Hot Start II DNA Polymerase (Thermo Scientific™) (the primers are listed in **Tables S5** and **S6**). The amplified coding sequences flanked by up- and downstream Golden Gate extensions were gel-purified using NucleoSpin™ Gel and PCR Clean-up kits (Marcherey-Nagel™), cloned into Plasmid PCR™-Blunt (Invitrogen™) and the resulting plasmids were isolated using the Nucleospin Plasmid™ kit (Marcherey-Nagel™). Compatible sets of sequenced (by Sigma-Aldrich and Eurofins) level 0 plasmids (promoter, CDS and terminator) were then assembled into a level 1 acceptor vector using a Golden Gate reaction with the enzyme *Bbs*I, leading to creation of a level 1 vector which contains a prokaryotic transcription unit (TU). In contrast to the level 0 vectors, the level 1 destination vectors (P12/P15/P23/P25/P34/P35/P45) confer chloramphenicol resistance, allowing efficient counter selection against level 0 vectors. The destination level 1 vectors contain a *lacZα* fragment flanked on each side by a *Bsa*I restriction site and two different Golden Gate extensions, making possible further directional cloning. The compatible level 1 vectors were employed for a second Golden Gate reaction using the enzyme *Bsa*I, leading to the creation of level 2 destination vectors that contain 1–4 TUs. Level 2 destination vectors confer resistance to apramycin (pOSV802m), hygromycin (pOSV808m) or kanamycin (pOSV811m), and encode a yellow color selectable marker (YFP from *Acropora millepora*). The vectors generated in this study are shown in **Table S6**.

The conjugation donor hosts *E. coli* ET12567/pUZ8002 or S17 were transformed with constructs for mobilization into *S. albus* J1074 and *S. lividans* TK24 strains, as previously described.[56] For each transformation, six independent exconjugants were plated onto TSA plates supplemented with appropriate antibiotics, and grown for 2−4 days until vegetative mycelia formed. The strains generated in this study are shown in **Table S7**.

Spectrophotometric Measurement of Glucuronidase Activity (GusA assay). We used a GusA assay adapted from that published by A. Luzhetskyy and colleagues.[42,57,58] For this, an X-Gluc stock solution was prepared in dimethyl sulfoxide to a final concentration of 0.1 mM. To qualitatively evaluate glucuronidase activity, 3-day-old plates of *S. albus* J1074 or *S. lividans* TK24 were flooded with 1 mL of 0.1 mM of X-Gluc and incubated at 30 °C for 1 h. For quantification, 100 µL of 48 h seed cultures of the *S. albus* J1074 and S*. lividans* TK24 recombinant strains were used to inoculate 10 mL of MYG liquid medium, which was incubated for 72 h. After cultivation, mycelia were gently sonicated to break up the pellets, then harvested by centrifugation (4,000*g* for 10 min), washed once with water, and resuspended in 500 µL of lysis buffer (50 mM phosphate buffer [pH 7.0], 1 mM tris(2-carboxyethyl) phosphine [TCEP], 0.1 % Triton X-100, 2 mg/mL lysozyme). Lysis was performed at 37 °C for 1 h, with mixing of the samples by inversion every 15 min. The lysates were centrifugated at 7,000*g* for 5 min. Then, 0.5 mL of lysate was mixed with 0.5 mL of dilution buffer (50 mM phosphate buffer [pH 7.0], 1 mM TCEP, 0.1 % Triton X-100) supplemented with 1 µL of 0.1 M of X-Gluc. The optical density at 615 nm ($OD_{615\ nm}$) was measured after 1 h of incubation at 30 °C. To determine the dry weight, a 1 mL aliquot of the culture was harvested by centrifugation (4,000*g* for 10 min), then the supernatant was carefully removed and the remaining pellet was dried for 48 h at 42 °C. The dried samples were then weighed. To calculate GusA activity, we employed the following equation: U/g = 20*A*/14*t*M,[57] where *A* = absorption at 615 nm, *t* = time in min and *M* = the dry weight in grams of the original sample size (1 mL). Microsoft Excel was used for statistical calculations. All data presented are means ± standard errors calculated from three independent experiments.

Growth Medium, Culture Conditions and Extraction. *S. albus* J1074 and *S. lividans* TK24 were grown on soya mannitol flour (SFM) agar plates for 5–7 days until well-sporulated. Spores from the agar plate were used to inoculate a seed culture of 10 mL malt yeast D-glucose (MYG) broth in a 125 mL Erlenmeyer shake flask and were grown for 48 h in an orbital shaker at 30 °C at 200 rpm. 200 µL of seed culture were used to inoculate 20 mL MYG liquid media in a 125 mL Erlenmeyer shake flask (1% *v*/*v* inoculum), and the culture fermented for 5 days at 200 rpm. Specialized metabolites were extracted from the culture supernatant twice with an equal volume of ethyl acetate + 0.1% formic acid. The samples were centrifuged at 16,000*g* for 5 minutes, dried under vacuum, resuspended in 250 µL of methanol and the solvent transferred to HPLC vials after filtration with a 0.22 µm filter.

LC-HRMS/MS-based Identification of Metabolites. Culture extracts were analyzed in both ESI positive and ESI negative ion modes (ESI^+ and ESI^-), and mass spectrometry conditions were as follows: spray voltage was set at +3.5 kV (ESI^+) and –2.5 kV (ESI^-); source gases were set (in arbitrary units/min) for sheath gas, auxiliary gas and sweep gas to 40, 8, and 1, respectively; vaporizer temperature was set to 320 °C and ion transfer tube temperature was set to 275 °C. Survey scans of precursors from 50–1000 *m/z* were performed at 60K resolution (full width of the peak at its half maximum, fwhm, at 200 *m/z*) with MS parameters as follows: RF-lens, 50%; maximum injection time, 50 ms; data type, profile; internal mass calibration EASY-IC TM activated; custom AGC target; normalized AGC target: 50%. A top speed (0.6 s) data-dependent MS^2 was performed by isolation at 1.5 Th with the quadrupole, HCD fragmentation with a stepped collision energy (15, 30, and 45) and MS analysis in the Orbitrap at 15K resolution (high resolution MS/MS analysis). Only the precursors with intensities above the threshold of 2.104 were sampled for MS^2. The dynamic exclusion duration was set to 2.5 s with a 10 ppm tolerance around the selected precursor (isotopes excluded). Other MS^2 parameters were as follows: data type, profile; custom AGC target; normalized AGC target: 20%. Mass spectrometer calibration was performed using the Pierce FlexMix calibration solution (Thermo Scientific). MS data acquisition was carried out utilizing the Xcalibur v. 3.0 software (Thermo Scientific).

■ ASSOCIATED CONTENT

Supporting Information

The supporting information is available free of charge at https://

DNA sequences of vectors; list of the genes, promoter and terminator parts (5′ → 3′) incorporating Golden Gate extensions that were cloned into Level 0 vectors; list of promoters and their origins; primers (5′ → 3′) used for promoter and terminator amplification used in this study; primers (5′ → 3′) used for modifying the *ncn* genes and for amplification of CDSs; list of constructed plasmids; bacterial strains used; summary of HPLC-ESI(+)-HRMS/MS data acquired in this study on *S. albus* strains; summary of HPLC-ESI(+)-HRMS/MS data acquired in this study *on* S. *lividans* strains; overview of level 0 to 2 vectors for MoClo application in Streptomyces; scheme of the GusA-based system for testing the various modular cloning cassettes; scheme of modular cloning level 1 plasmids; modular cloning level 2 plasmids used for assembling the napthocyclinone (Ncn) genetic circuit; HPLC-ESI(+)-HRMS/MS analysis of mutactin **8a**, dehydro-mutactin **8b**, Sek4 **6a**/Sek4b **7a**, dehydro-Sek4 **6b**, dehydro-Sek4b **7b**, flavokermesic acid **1** and kermesic acid **4**; metabolic profile of a commercial extract of carminic acid.

■ AUTHOR INFORMATION

Corresponding author

Kira J. Weissman – *Université de Lorraine, CNRS, IMoPA, F-54000 Nancy, France*; https://orcid.org/0000-0002-3012-2960; E-mail: kira.weissman@univ-lorraine.fr

Authors

Jean-Malo Massicard – *Université de Lorraine, CNRS, IMoPA, F-54000 Nancy, France*

Delphine Noel – *Université de Lorraine, CNRS, IMoPA, F-54000 Nancy, France*

Andrea Calderari – *Université de Lorraine, CNRS, IMoPA, F-54000 Nancy, France*

André Le Jeune – *Abolis Biotechnologies, 5 Rue Henri Auguste Desbruères Bâtiment 6, 91000, Évry, France*

Cyrille Pauthenier – *Abolis Biotechnologies, 5 Rue Henri Auguste Desbruères Bâtiment 6, 91000, Évry, France*

Author Contributions

The research study was conceived by K.J.W and J-M.M. Molecular biological work was designed by J-M.M., A.L.J. and C.P., and conducted by J-M.M, D.N and A.C. The analytical chemistry was carried out by J-M.M and K.J.W. The manuscript was written by J-M.M. and K.J.W., and approved by all authors.

Notes

Conflicts of interest: none.

■ ACKNOWLEDGEMENTS

We are grateful to the Agence National de la Recherche (ANR) for financial support via grant AnthraLab/ANR-21-LCV1-0008 (to K.J.W.), C. Paris of the Plateau Commun Analyse Structurale et Métabolomique (PASM) for acquisition of the LC-HRMS/MS data. C. Jacob (UL) is thanked for helpful discussions.

■ REFERENCES

(1) Myronovskyi, M.; Luzhetskyy, A. Heterologous Production of Small Molecules in the Optimized *Streptomyces* Hosts. *Nat. Prod. Rep.* **2019**, *36* (9), 1281–1294.

(2) Phelan, R. M.; Sachs, D.; Petkiewicz, S. J.; Barajas, J. F.; Blake-Hedges, J. M.; Thompson, M. G.; Reider Apel, A.; Rasor, B. J.; Katz, L.; Keasling, J. D. Development of Next Generation Synthetic Biology Tools for Use in *Streptomyces venezuelae*. *ACS. Synth. Biol.* **2017**, *6* (1), 159–166.

(3) Liu, R.; Deng, Z.; Liu, T. *Streptomyces* Species: Ideal Chassis for Natural Product Discovery and Overproduction. *Metab. Eng.* **2018**, *50*, 74–84.

(4) Wang, R.; Nguyen, J.; Hecht, J.; Schwartz, N.; Brown, K. V.; Ponomareva, L. V.; Niemczura, M.; van Dissel, D.; van Wezel, G. P.; Thorson, J. S.; Metsä-Ketelä, M.; Shaaban, K. A.; Nybo, S. E. A BioBricks Metabolic Engineering Platform for the Biosynthesis of Anthracyclinones in *Streptomyces coelicolor*. *ACS Synth. Biol.* **2022**, *11* (12), 4193–4209.

(5) Zhu, X.; Siitonen, V.; Melançon Iii, C. E.; Metsä-Ketelä, M. Biosynthesis of Diverse Type II Polyketide Core Structures in *Streptomyces coelicolor* M1152. *ACS Synth. Biol.* **2021**, *10* (2), 243–251.

(6) Summers, R. G.; Ali, A.; Shen, B.; Wessel, W. A.; Hutchinson, C. R. Malonyl-Coenzyme A:Acyl Carrier Protein Acyltransferase of *Streptomyces glaucescens*: A Possible Link between Fatty Acid and Polyketide Biosynthesis. *Biochemistry* **1995**, *34* (29), 9389–9402.

(7) Javidpour, P.; Bruegger, J.; Srithahan, S.; Korman, T. P.; Crump, M. P.; Crosby, J.; Burkart, M. D.; Tsai, S.-C. The Determinants of Activity and Specificity in Actinorhodin Type II Polyketide Ketoreductase. *Chem. Biol.* **2013**, *20* (10), 1225–1234.

(8) Engler, C.; Kandzia, R.; Marillonnet, S. A One Pot, One Step, Precision Cloning Method with High Throughput Capability. *PLoS One* **2008**, *3* (11).

(9) Weber, E.; Engler, C.; Gruetzner, R.; Werner, S.; Marillonnet, S. A Modular Cloning System for Standardized Assembly of Multigene Constructs. *PLoS One* **2011**, *6* (2), e16765.

(10) Sarrion-Perdigones, A.; Falconi, E. E.; Zandalinas, S. I.; Juárez, P.; Fernández-del-Carmen, A.; Granell, A.; Orzaez, D. GoldenBraid: An Iterative Cloning System for Standardized Assembly of Reusable Genetic Modules. *PLoS One* **2011**, *6* (7), e21622.

(11) Schmidt, M.; Lee, N.; Zhan, C.; Roberts, J. B.; Nava, A. A.; Keiser, L. S.; Vilchez, A. A.; Chen, Y.; Petzold, C. J.; Haushalter, R. W.; Blank, L. M.; Keasling, J. D. Maximizing Heterologous Expression of Engineered Type I Polyketide Synthases: Investigating Codon Optimization Strategies. *ACS Synth. Biol.* **2023**, *12* (11), 3366–3380.

(12) Wang, R.; Nji Wandi, B.; Schwartz, N.; Hecht, J.; Ponomareva, L.; Paige, K.; West, A.; Desanti, K.; Nguyen, J.; Niemi, J.; Thorson, J. S.; Shaaban, K. A.; Metsä-Ketelä, M.; Nybo, S. E. Diverse Combinatorial Biosynthesis Strategies for C-H Functionalization of Anthracyclinones. *ACS Synth. Biol.* **2024**, *13* (5), 1523–1536.

(13) Silva-Rocha, R.; Martínez-García, E.; Calles, B.; Chavarría, M.; Arce-Rodríguez, A.; de Las Heras, A.; Páez-Espino, A. D.; Durante-Rodríguez, G.; Kim, J.; Nikel, P. I.; Platero, R.; de Lorenzo, V. The Standard European Vector Architecture (SEVA): A Coherent Platform for the Analysis and Deployment of Complex Prokaryotic Phenotypes. *Nucleic Acids Res.* **2013**, *41*, D666–675.

(14) Magadán-Corpas, P.; Ye, S.; Pérez-Valero, Á.; McAlpine, P. L.; Valdés-Chiara, P.; Torres-Bacete, J.; Nogales, J.; Villar, C. J.; Lombó, F. Optimized *De Novo* Eriodictyol Biosynthesis in *Streptomyces albidoflavus* Using an Expansion of the Golden Standard Toolkit for Its Use in Actinomycetes. *Int. J. Mol. Sci.* **2023**, *24* (10), 8879.

(15) Aubry, C.; Pernodet, J.-L.; Lautru, S. Modular and Integrative Vectors for Synthetic Biology Applications in *Streptomyces* Spp. *Appl. Environ. Microbiol.* **2019**, *85* (16).

(16) Tang, Y.; Lee, T. S.; Khosla, C. Engineered Biosynthesis of Regioselectively Modified Aromatic Polyketides Using Bimodular Polyketide Synthases. *PLoS Biol.* **2004**, *2* (2), E31.

(17) Cummings, M.; Peters, A. D.; Whitehead, G. F. S.; Menon, B. R. K.; Micklefield, J.; Webb, S. J.; Takano, E. Assembling a Plug-and-Play Production Line for Combinatorial Biosynthesis of Aromatic Polyketides in *Escherichia coli*. *PLoS Biol.* **2019**, *17* (7), e3000347.

(18) Brachmann, A. O.; Joyce, S. A.; Jenke-Kodama, H.; Schwär, G.; Clarke, D. J.; Bode, H. B. A Type II Polyketide Synthase Is Responsible for Anthraquinone Biosynthesis in *Photorhabdus luminescens*. *ChemBioChem* **2007**, *8* (14), 1721–1728.

(19) Yang, D.; Jang, W. D.; Lee, S. Y. Production of Carminic Acid by Metabolically Engineered *Escherichia coli*. *J. Am. Chem. Soc.* **2021**, *143* (14), 5364–5377.

(20) Li, Y.; Xu, Z.; Chen, P.; Zuo, C.; Chen, L.; Yan, W.; Jiao, R.; Ye, Y. Genome Mining and Heterologous Expression Guided the Discovery of Antimicrobial Naphthocyclinones from *Streptomyces eurocidicus* CGMCC 4.1086. *J. Agric. Food Chem.* **2023**, *71* (6), 2914–2923.

(21) Brünker, P.; McKinney, K.; Sterner, O.; Minas, W.; Bailey, J. E. Isolation and Characterization of the Naphthocyclinone Gene Cluster from *Streptomyces arenae* DSM 40737 and Heterologous Expression of the Polyketide Synthase Genes. *Gene* **1999**, *227* (2), 125–135.

(22) Eisner, T.; Nowicki, S.; Goetz, M.; Meinwald, J. Red Cochineal Dye (Carminic Acid): Its Role in Nature. *Science* **1980**, *208* (4447), 1039–1042.

(23) Rasmussen, S. A.; Kongstad, K. T.; Khorsand-Jamal, P.; Kannangara, R. M.; Nafisi, M.; Van Dam, A.; Bennedsen, M.; Madsen, B.; Okkels, F.; Gotfredsen, C. H.; Staerk, D.; Thrane, U.; Mortensen, U. H.; Larsen, T. O.; Frandsen, R. J. N. On the Biosynthetic Origin of Carminic Acid. *Insect Biochem. Mol. Biol.* **2018**, *96*, 51–61.

(24) Kannangara, R.; Siukstaite, L.; Borch-Jensen, J.; Madsen, B.; Kongstad, K. T.; Staerk, D.; Bennedsen, M.; Okkels, F. T.; Rasmussen, S. A.; Larsen, T. O.; Frandsen, R. J. N.; Møller, B. L. Characterization of a Membrane-Bound *C*-Glucosyltransferase Responsible for Carminic Acid Biosynthesis in *Dactylopius coccus Costa*. *Nat. Commun.* **2017**, *8* (1), 1987.

(25) Frandsen, R. J. N.; Khorsand-Jamal, P.; Kongstad, K. T.; Nafisi, M.; Kannangara, R. M.; Staerk, D.; Okkels, F. T.; Binderup, K.; Madsen, B.; Møller, B. L.; Thrane, U.; Mortensen, U. H. Heterologous Production of the Widely Used Natural Food Colorant Carminic Acid in *Aspergillus nidulans*. *Sci. Rep.* **2018**, *8* (1), 12853.

(26) Ames, B. D.; Lee, M.-Y.; Moody, C.; Zhang, W.; Tang, Y.; Tsai, S.-C. Structural and Biochemical Characterization of ZhuI Aromatase/Cyclase from the R1128 Polyketide Pathway. *Biochemistry* **2011**, *50* (39), 8392–8406.

(27) McDaniel, R.; Ebert-Khosla, S.; Hopwood, D. A.; Khosla, C. Engineered Biosynthesis of Novel Polyketides. *Science* **1993**, *262* (5139), 1546–1550.

(28) Ahmed, Y.; Rebets, Y.; Estévez, M. R.; Zapp, J.; Myronovskyi, M.; Luzhetskyy, A. Engineering of *Streptomyces lividans* for Heterologous Expression of Secondary Metabolite Gene Clusters. *Microb. Cell Fact.* **2020**, *19* (1), 5.

(29) Taguchi, T.; Itou, K.; Ebizuka, Y.; Malpartida, F.; Hopwood, D. A.; Surti, C. M.; Booker-Milburn, K. I.; Stephenson, G. R.; Ichinose, K. Chemical Characterisation of Disruptants of the *Streptomyces coelicolor* A3(2) actVI Genes Involved in Actinorhodin Biosynthesis. *J. Antibiot.* **2000**, *53* (2), 144–152.

(30) Nagai, T.; Ibata, K.; Park, E. S.; Kubota, M.; Mikoshiba, K.; Miyawaki, A. A Variant of Yellow Fluorescent Protein with Fast and Efficient Maturation for Cell-Biological Applications. *Nat. Biotechnol.* **2002**, *20* (1), 87–90.

(31) Bai, C.; Zhang, Y.; Zhao, X.; Hu, Y.; Xiang, S.; Miao, J.; Lou, C.; Zhang, L. Exploiting a Precise Design of Universal Synthetic Modular Regulatory Elements to Unlock the Microbial Natural Products in *Streptomyces*. *Proc. Natl. Acad. Sci. U. S. A.* **2015**, *112* (39), 12181–12186.

(32) Ji, C.-H.; Kim, J.-P.; Kang, H.-S. Library of Synthetic Streptomyces Regulatory Sequences for Use in Promoter Engineering of Natural Product Biosynthetic Gene Clusters. *ACS Synth. Biol.* **2018**, *7* (8), 1946–1955.

(33) Luo, Y.; Zhang, L.; Barton, K. W.; Zhao, H. Systematic Identification of a Panel of Strong Constitutive Promoters from *Streptomyces albus*. *ACS Synth. Biol.* **2015**, *4* (9), 1001–1010.

(34) Shao, Z.; Rao, G.; Li, C.; Abil, Z.; Luo, Y.; Zhao, H. Refactoring the Silent Spectinabilin Gene Cluster Using a Plug-and-Play Scaffold. *ACS Synth. Biol.* **2013**, *2* (11), 662–669.

(35) Zhao, M.; Wang, S.-L.; Tao, X.-Y.; Zhao, G.-L.; Ren, Y.-H.; Wang, F.-Q.; Wei, D.-Z. Engineering Diverse Eubacteria Promoters for Robust Gene Expression in *Streptomyces lividans*. *J. Biotechnol.* **2019**, *289*, 93–102.

(36) Cobb, R. E.; Wang, Y.; Zhao, H. High-Efficiency Multiplex Genome Editing of *Streptomyces* Species Using an Engineered CRISPR/Cas System. *ACS Synth. Biol.* **2015**, *4* (6), 723–728.

(37) Bednarz, B.; Kotowska, M.; Pawlik, K. J. Multi-Level Regulation of Coelimycin Synthesis in *Streptomyces coelicolor* A3(2). *Appl. Microbiol. Biotechnol.* **2019**, *103* (16), 6423–6434.

(38) Gottelt, M.; Kol, S.; Gomez-Escribano, J. P.; Bibb, M.; Takano, E. Deletion of a Regulatory Gene within the *Cpk* Gene Cluster Reveals Novel Antibacterial Activity in *Streptomyces coelicolor* A3(2). *Microbiology* **2010**, *156* (Pt 8), 2343–2353.

(39) Wang, W.; Li, X.; Wang, J.; Xiang, S.; Feng, X.; Yang, K. An Engineered Strong Promoter for Streptomycetes. *Appl. Environ. Microbiol.* **2013**, *79* (14), 4484–4492.

(40) Tong, Y.; Charusanti, P.; Zhang, L.; Weber, T.; Lee, S. Y. CRISPR-Cas9 Based Engineering of Actinomycetal Genomes. *ACS Synth. Biol.* **2015**, *4* (9), 1020–1029.

(41) Hopwood, D. A. Highlights of *Streptomyces* Genetics. *Heredity* **2019**, *123* (1), 23–32.

(42) Horbal, L.; Siegl, T.; Luzhetskyy, A. A Set of Synthetic Versatile Genetic Control Elements for the Efficient Expression of Genes in Actinobacteria. *Sci. Rep.* **2018**, *8* (1), 491.

(43) Ciampi, M. S. Rho-Dependent Terminators and Transcription Termination. *Microbiology* **2006**, *152* (Pt 9), 2515–2528.

(44) Reynolds, R.; Chamberlin, M. J. Parameters Affecting Transcription Termination by *Escherichia coli* RNA. II. Construction and Analysis of Hybrid Terminators. *J. Mol. Biol.* **1992**, *224* (1), 53–63.

(45) Chen, Y.-J.; Liu, P.; Nielsen, A. A. K.; Brophy, J. A. N.; Clancy, K.; Peterson, T.; Voigt, C. A. Characterization of 582 Natural and Synthetic Terminators and Quantification of Their Design Constraints. *Nat. Methods* **2013**, *10* (7), 659–664.

(46) Marti, T.; Hu, Z.; Pohl, N. L.; Shah, A. N.; Khosla, C. Cloning, Nucleotide Sequence, and Heterologous Expression of the Biosynthetic Gene Cluster for R1128, a Non-Steroidal Estrogen Receptor Antagonist. Insights into an Unusual Priming Mechanism. *J. Biol. Chem.* **2000**, *275* (43), 33443–33448.

(47) McDaniel, R.; Ebert-Khosla, S.; Fu, H.; Hopwood, D. A.; Khosla, C. Engineered Biosynthesis of Novel Polyketides: Influence of a Downstream Enzyme on the Catalytic Specificity of a Minimal Aromatic Polyketide Synthase. *Proc. Natl. Acad. Sci. U. S. A.* **1994**, *91* (24), 11542–11546.

(48) Zhang, Q.; Wang, X.; Zeng, W.; Xu, S.; Li, D.; Yu, S.; Zhou, J. De Novo Biosynthesis of Carminic Acid in *Saccharomyces cerevisiae*. *Metab. Eng.* **2023**, *76*, 50–62.

(49) Fu, H.; Hopwood, D. A.; Khosla, C. Engineered Biosynthesis of Novel Polyketides: Evidence for Temporal, but Not Regiospecific, Control of Cyclization of an Aromatic Polyketide Precursor. *Chem. Biol.* **1994**, *1* (4), 205–210.

(50) Hashimoto, M.; Taguchi, T.; Ishikawa, K.; Mori, R.; Hotta, A.; Watari, S.; Katakawa, K.; Kumamoto, T.; Okamoto, S.; Ichinose, K. Unveiling Two Consecutive Hydroxylations: Mechanisms of Aromatic Hydroxylations Catalyzed by Flavin-Dependent Monooxygenases for the Biosynthesis of Actinorhodin and Related Antibiotics. *ChemBioChem* **2020**, *21* (5), 623–627.

(51) Baral, B.; Matroodi, S.; Siitonen, V.; Thapa, K.; Akhgari, A.; Yamada, K.; Nuutila, A.; Metsä-Ketelä, M. Co-Factor Independent Oxidases ncnN and actVA-3 Are Involved in the Dimerization of Benzoisochromanequinone Antibiotics in Naphthocyclinone and Actinorhodin Biosynthesis. *FEMS Microbiol. Lett.* **2023**, *370*, fnad123.

(52) Brünke, P.; Sterner, O.; Bailey, J. E.; Minas, W. Heterologous Expression of the Naphthocyclinone Hydroxylase Gene from *Streptomyces arenae* for Production of Novel Hybrid Polyketides. *Antonie Van Leeuwenhoek* **2001**, *79* (3–4), 235–245.

(53) Caldara-Festin, G.; Jackson, D. R.; Barajas, J. F.; Valentic, T. R.; Patel, A. B.; Aguilar, S.; Nguyen, M.; Vo, M.; Khanna, A.; Sasaki, E.; Liu, H.-W.; Tsai, S.-C. Structural and Functional Analysis of Two Di-Domain Aromatase/Cyclases from Type II Polyketide Synthases. *Proc. Natl. Acad. Sci. U. S. A.* **2015**, *112* (50), E6844-6851.

(54) Li, L.; MacIntyre, L. W.; Brady, S. F. Refactoring Biosynthetic Gene Clusters for Heterologous Production of Microbial Natural Products. *Curr. Opin. Biotechnol.* **2021**, *69*, 145–152.

(55) Scherlach, K.; Hertweck, C. Mining and Unearthing Hidden Biosynthetic Potential. *Nat. Commun.* **2021**, *12* (1), 3864.

(56) Tong, Y.; Whitford, C. M.; Blin, K.; Jørgensen, T. S.; Weber, T.; Lee, S. Y. CRISPR-Cas9, CRISPRi and CRISPR-BEST-Mediated Genetic Manipulation in *Streptomycetes*. *Nat. Protoc.* **2020**, *15* (8), 2470–2502.

(57) Horbal, L.; Fedorenko, V.; Luzhetskyy, A. Novel and Tightly Regulated Resorcinol and Cumate-Inducible Expression Systems for *Streptomyces* and Other Actinobacteria. *Appl. Microbiol. Biotechnol.* **2014**, *98* (20), 8641–8655.

(58) Myronovskyi, M.; Welle, E.; Fedorenko, V.; Luzhetskyy, A. β-Glucuronidase as a Sensitive and Versatile Reporter in Actinomycetes. *Appl. Environ. Microbiol.* **2011**, *77* (15), 5370–5383.

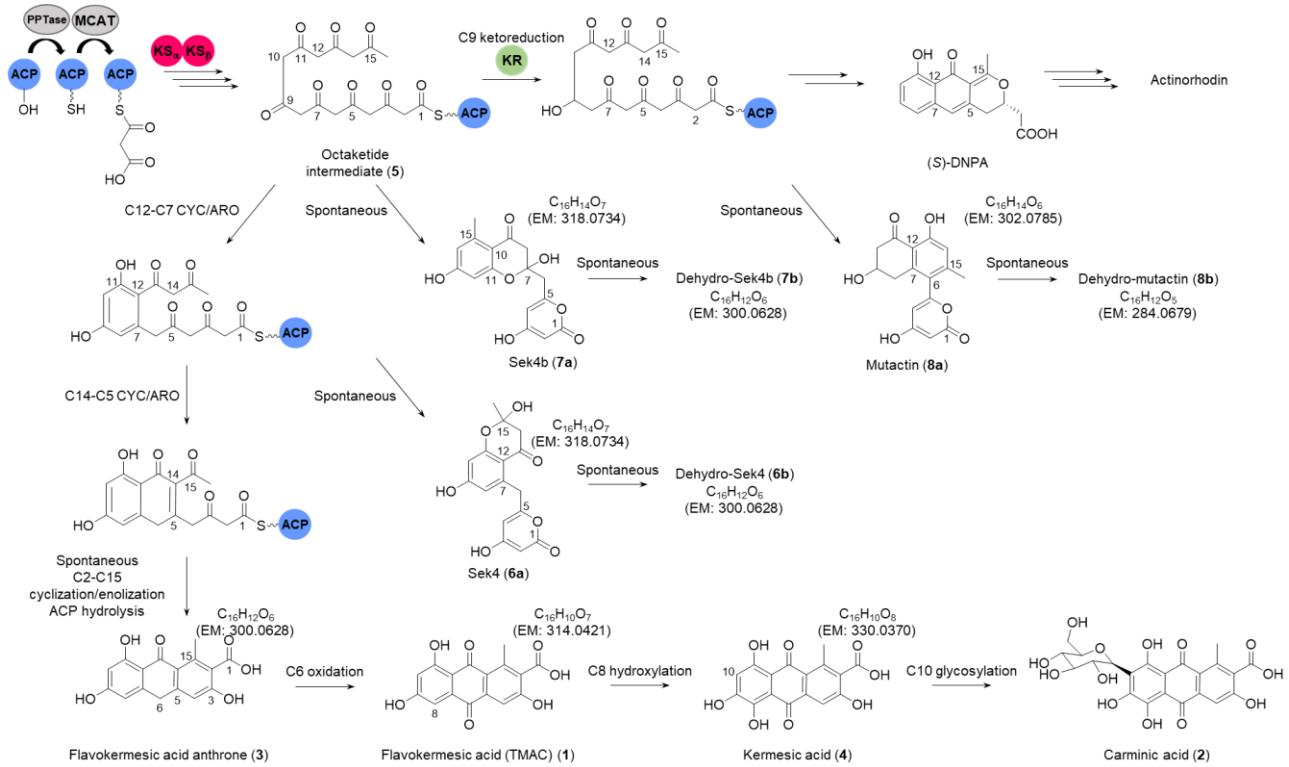

Figure 1. Proposed biosynthetic pathway to kermesic acid **4** in *Streptomyces* via introduction of heterologous type II PKSs and ARO/CYC enzymes ZhuI and ZhuJ. In *S. lividans* TK24, C-6 oxidation may occur spontaneously, while both C-6 and C-8 oxidation may be catalyzed by an endogenous hydroxylase present in the strain. The C-10 glycosylation step to yield carminic acid **2** has not been addressed in this work. Metabolites Sek4 **6a**, Sek4b **7a** and their dehydrated equivalents (**6b**/**7b**) arise from spontaneous chemistry on pathway intermediates. Shunting towards mutactin **8a**/dehydro-mutactin **8b** in *S. lividans* occurs following C-9 ketoreduction, presumably catalyzed by the Act KR.

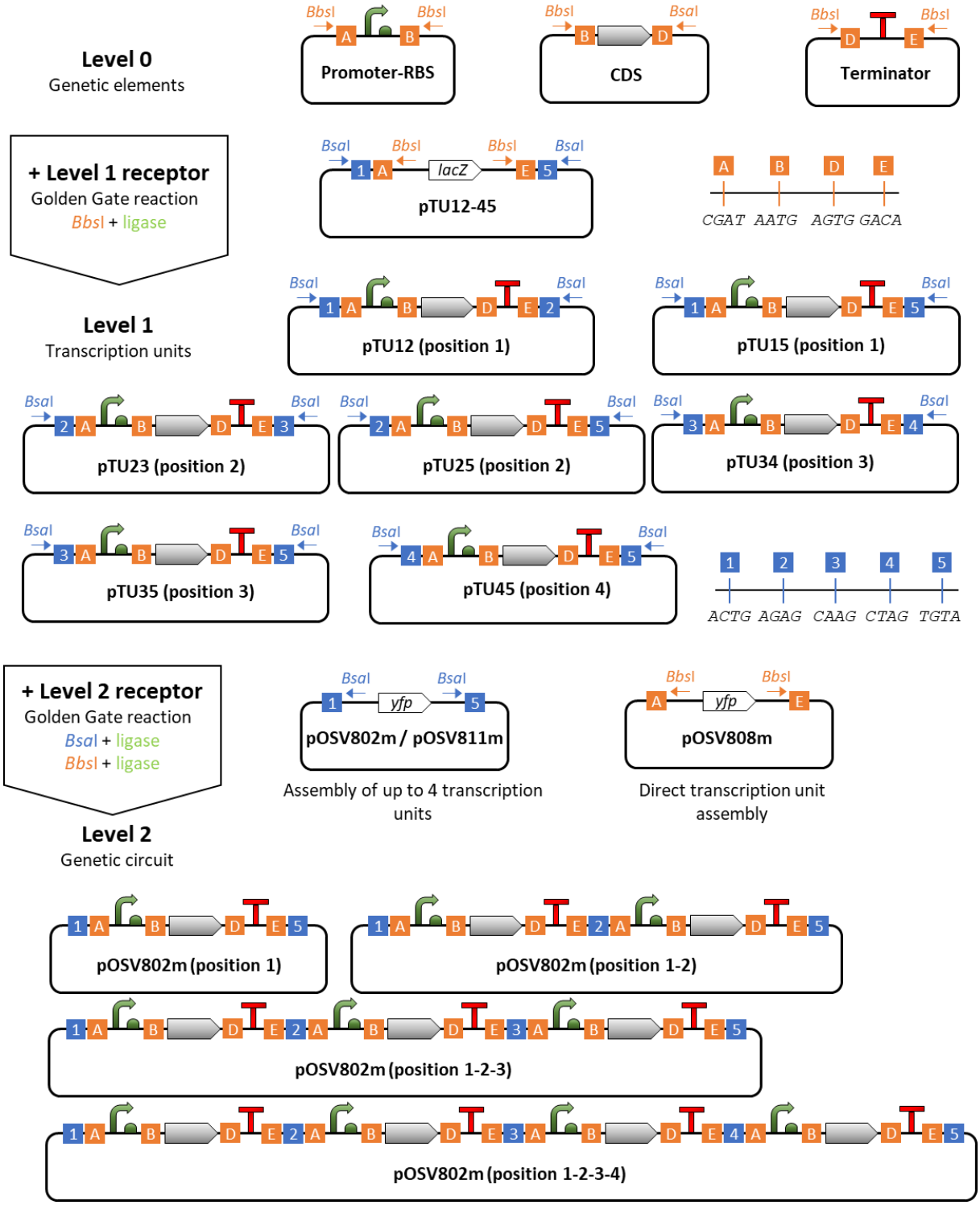

Figure 2. Hierarchy and graphical description of modular cloning assembly. The MoClo hierarchy ranges from genetic elements (level 0) that are assembled to generate transcription units (level 1), which in turn can be assembled into complex genetic circuits (level 2). A modular cloning reaction consists of a series of restriction/ligation cycles whose operation is the same, irrespective of the level under construction. Restriction steps release the genetic features flanked by the corresponding Type IIS recognition sites (*Bbs*I or *Bsa*I), and remove the *lacZ* or *yfp* gene from the receptor vector. The ligation steps result in assembly of the genetic features in a pre-defined order into the receptor vector.

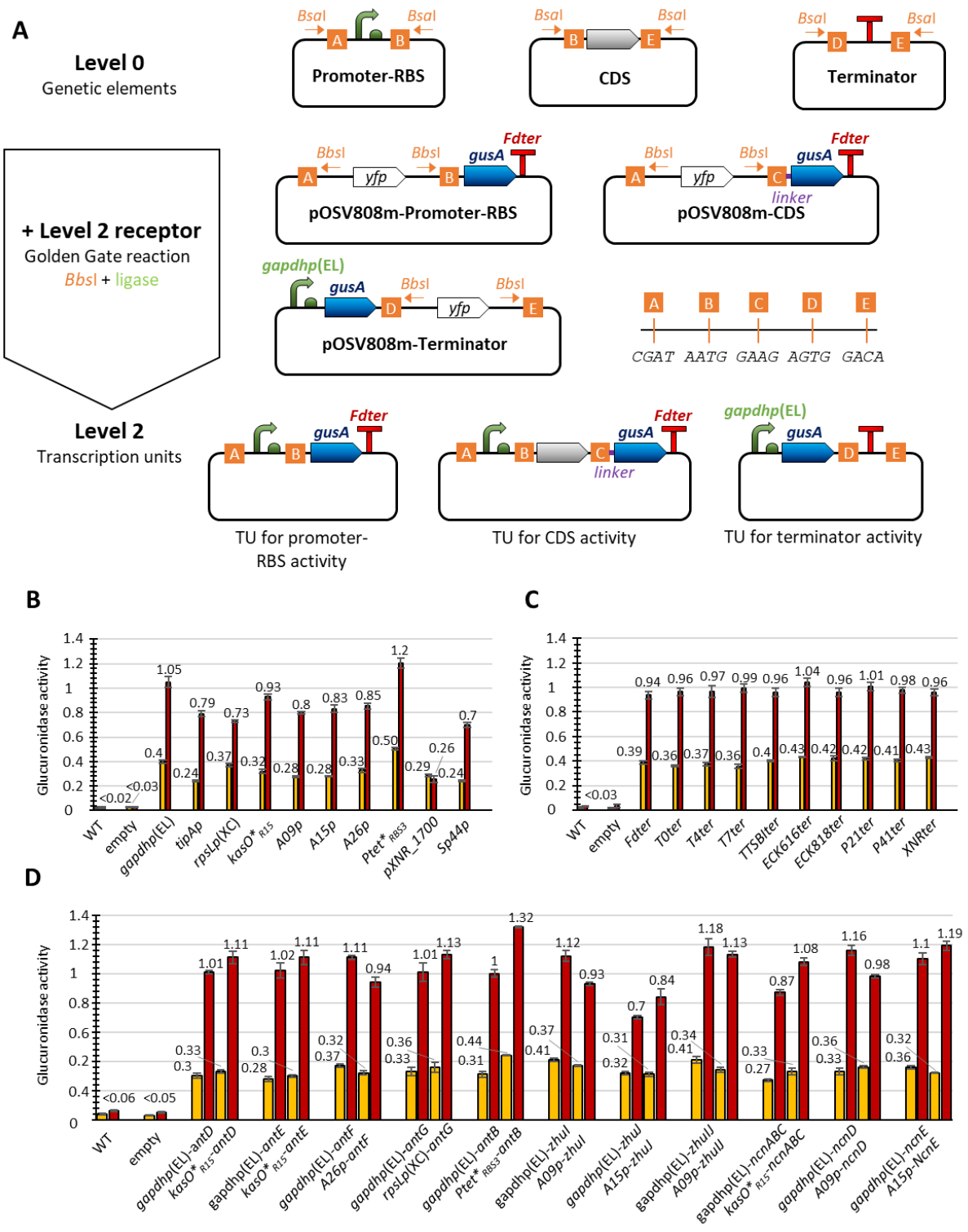

Figure 3. Hierarchy and validation of the genetic elements. (A) Hierarchy of modular cloning assembly in combination with GusA essay for testing the functionality of (B) promoters-RBS, (C) terminators, and (D) promoter-RBS in combination with CDS in *Streptomyces albus* J1074 (yellow) and *Streptomyces lividans* TK24 (red). Glucuronidase (GusA) activity in cell lysates of *S. lividans* TK24 and *S. albus* J1074 was evaluated after 3 days of growth in MYG medium via measurement of the absorbance ($OD_{615\ nm}$) normalized to the dry biomass. The data are reported as mean ± s.d. from three independent experiments.

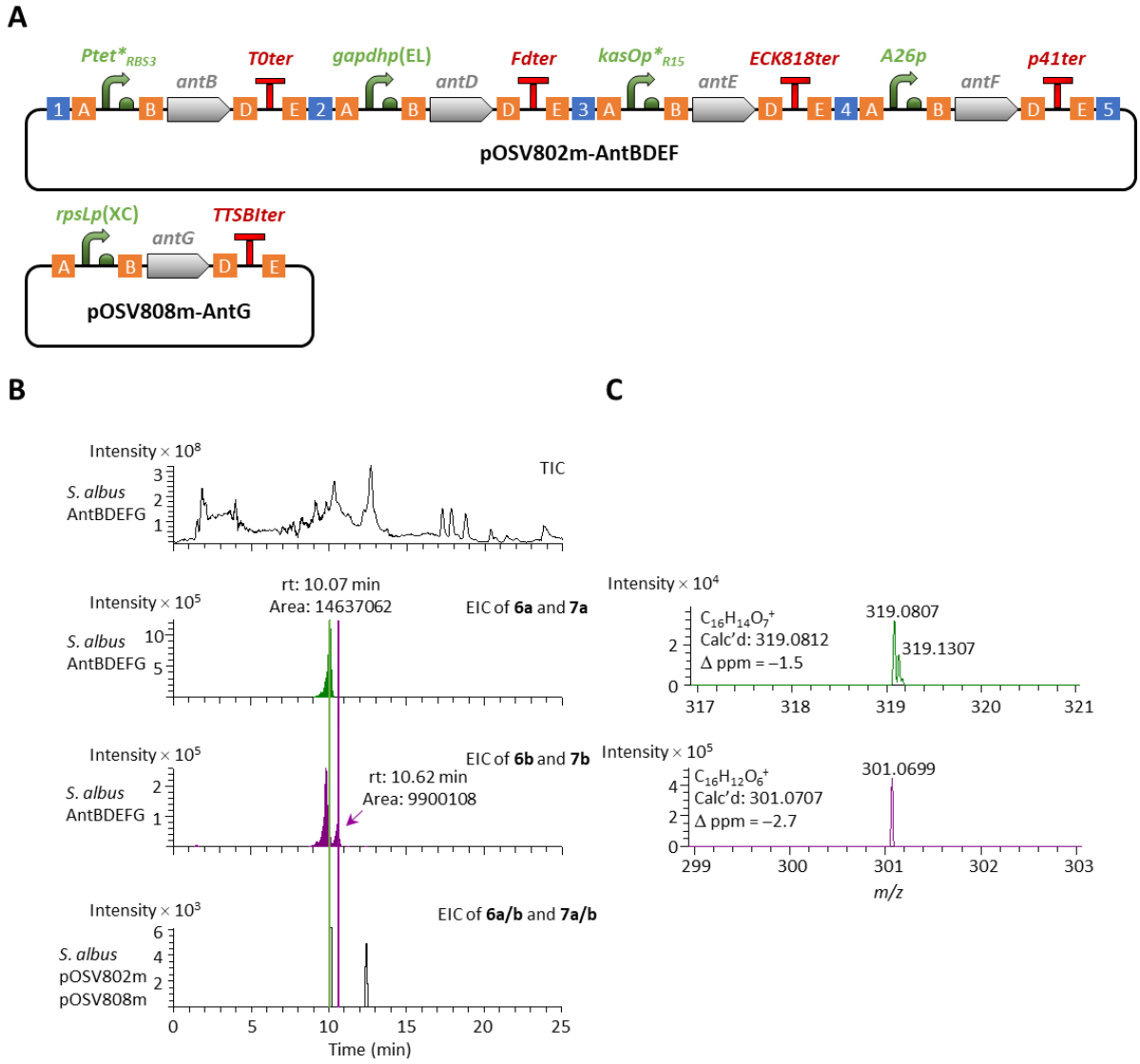

Figure 4. Metabolic profile of *S. albus* J1074 expression strains containing heterologous *ant* genes. (A) Level 2 plasmids used to introduce the Ant minPKS, alongside AntB (phosphopantetheinyl transferase) and AntG (CoA-ligase). (B) Extracted ion chromatograms (EICs) from LC-HRMS performed in positive ion mode, based on the calculated exact masses (*m*/*z* $[M+H]^+$) for Sek4 **6a**/Sek4b **7a** (319.0812) and dehydro-Sek4 **6b**/Sek4b **7b** (301.0707). The first three chromatograms represent the *S. albus* J1074 strain transformed with the plasmids, and the last, *S. albus* J1074 transformed with empty plasmid. The first peak in the EIC of **6b**/**7b** (r.t. 10.07 min) likely represents **6b**/**7b** derived from **6a**/**7a** by dehydration during MS analysis. While no separation was achieved in this analysis between the peaks corresponding to **6b** and **7b**, other runs produced distinct peaks, which allowed for acquisition of MS^2 data on the two compounds (the MS^2 data for **6ab** and **7ab** are provided in **Figures S7**–**S9**). TIC, total ion chromatogram. (C) Measured exact masses for the metabolites shown in (B).

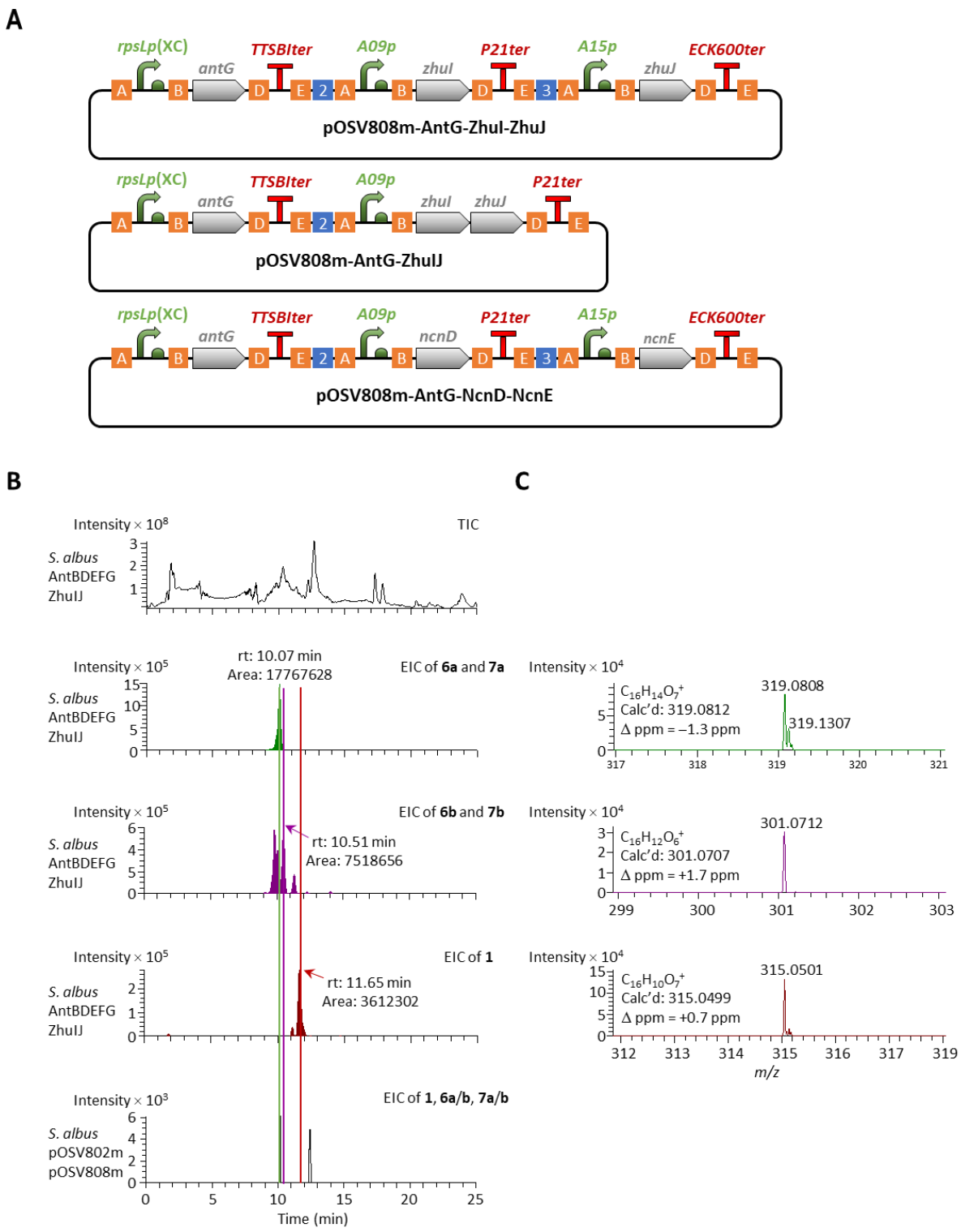

Figure 5. Metabolic profile of *S. albus* J1074 expression strains containing the Ant minPKS in combination with Zhu and Ncn ARO/CYC. (**A**) Level 2 plasmids used to introduce AntG and the cyclase pairs into the *S. albus* strain expressing the Ant minPKS and AntB. (B) Extracted ion chromatograms (EICs) from LC-HRMS performed in positive ion mode, based on the calculated masses (*m/z* $[M+H]^+$) for Sek4 **6a**/Sek4b **7a** (319.0812), dehydro-Sek4 **6b**/Sek4b **7b** (301.0707) and flavokermesic acid **1** (315.0499)). The first four chromatograms represent the *S. albus* J1074 strain transformed with the plasmids, and the last, *S. albus* J1074 transformed with empty plasmid. TIC, total ion chromatogram. (C) Measured exact masses for the metabolites shown in (B). Accompanying MS^2 data for **1**, **6ab** and **7ab** are provided in **Figures S7**–**S9**, and **S11**.